Applied Catalysis B: Environmental 132–133 (2013) 401–407

Contents lists available at SciVerse ScienceDirect

Applied Catalysis B: Environmental

journal homepage: www.elsevier.com/locate/apcatb

Heterogeneous catalytic reaction of elemental mercury vapor over cupric chloride for mercury emissions control

Xin Li, Zhouyang Liu, Jinsoo Kim, Joo-Youp Lee*

Chemical Engineering Program, School of Energy, Environmental, Biological, and Medical Engineering, University of Cincinnati, Cincinnati, OH 45221-0012, United States

ARTICLE INFO

Article history:
Received 13 August 2012
Received in revised form
15 November 2012
Accepted 21 November 2012
Available online 29 November 2012

Keywords:
Elemental mercury oxidation
Cupric chloride
Redox catalyst
Coal combustion flue gas

ABSTRACT

In this study, the reaction mechanism of Hg(0) vapor oxidation over cupric chloride ($CuCl_2$) was investigated using 10% (wt) $CuCl_2$/α-Al_2O_3 for mercury emissions control from coal-fired power plants. The $CuCl_2$/α-Al_2O_3 sample showed >90% Hg(0) oxidation with excellent resistance to SO_2 at 140 °C in a simulated flue gas containing 10 ppmv HCl, 2000 ppmv SO_2, and 6% O_2 gases balanced with N_2 gas. In the absence of HCl and O_2 gases, Hg(0) vapor was found to be oxidized by consuming atomic Cl of $CuCl_2$ and reducing it to CuCl, following a Mars–Maessen mechanism. The reduced CuCl could be re-chlorinated back to $CuCl_2$ by replenishing empty Cl atoms under 10 ppmv HCl and 6% O_2 gases readily present in coal combustion flue gases even under 2000 ppmv SO_2 concentration for continuous Hg(0) oxidation. Cl_2 gas generation was not observed over $CuCl_2$ at 140 °C, indicating a heterogeneous catalytic reaction. $CuCl_2$ shows potential that can be realized in a honeycomb or plate catalyst bed.

© 2012 Elsevier B.V. All rights reserved.

1. Introduction

On December 21, 2011, the U.S. Environmental Protection Agency (EPA) announced the Mercury and Air Toxics Standards (MATS) rule that would limit mercury, acid gases, and other toxic heavy metal emissions from coal- and oil-fired utility, industrial, commercial, and institutional power plants [1]. The new rule, which was effective on April 16, 2012, will reduce mercury emissions by >90%. In July 2010 prior to the MATS, the U.S. EPA also issued a new proposed rule, the Transport Rule, which replaces the 2005 Clean Air Interstate Rule (CAIR) and will start to regulate sulfur dioxide (SO_2) and nitrogen oxide (NO_x) emissions from power plants in 28 states from 2012 [2,3]. The U.S. EPA estimates that a total 272.2 GW of flue gas desulfurization (FGD) and 217.6 GW of selective catalytic reduction (SCR) units of a total 373 GW to be generated from coal combustion would be operative by 2020 in order to meet the Transport Rule requirements (according to the TR SB Limited Trading model) [4].

The use of powder river basin (PRB) subbituminous coal, which generates higher percentages of elementary mercury (Hg(0)) vapor, is increasing [5], and the proposed Transport Rule is very likely to increase the installation of wet FGD systems (>95% for SO_2 control on a basis of total electricity generation) and SCR units for large coal-fired power plants. In this context, heterogeneous Hg(0) oxidation using catalysts or oxidants is highly expected to play a critical role in future mercury emissions control in the U.S. [6–8]. Among these oxidized mercury species, $HgCl_2$ has high solubility in water (i.e. 7.37 g/100 g water at 25 °C) and other oxidized forms have very low solubility [9]. Therefore, $HgCl_2$ is the most desirable oxidized form for capture in wet FGD systems and is proven to be removable by activated carbon injection.

To date, noble metals and metal oxides have been primarily studied for heterogeneous catalytic Hg(0) oxidation. Noble metal-based catalysts have shown limited success in the absence of HCl or Cl_2 gas [7,10–12]. Au and Pd catalysts oxidize Hg(0) vapor primarily by Cl_2 gas, but Pt catalyst requires HCl and O_2 gases for Hg(0) oxidation, suggesting different mechanisms [10–12]. Recently, various metal oxide-based Hg(0) catalysts including V_2O_5, MoO_3, Cr_2O_3, MnO_x, CeO_2, Co_3O_4 and RuO_2 have been studied for the development of a Hg(0)-specific or modified SCR catalyst [13–19]. However, even in the presence of HCl gas, many of these metal oxide catalysts exhibited limited Hg(0) oxidation at a low HCl level typically found in subbituminous or lignite coal combustion flue gas (e.g. ≤10 ppm) due to the competitive adsorption of multiple gases including SO_2, NH_3, HCl, and Hg(0) onto metal oxide sites. The Deacon reaction shown in reaction (1) producing Cl_2 gas from HCl and O_2 gases over V_2O_5, MnO_x, and RuO_2 was proposed to correlate with Hg(0) oxidation [14,16,20]. However, the homogeneous reaction between Cl_2 gas and Hg(0) vapor is known to be slow, and is not enough to explain the extent of observed Hg(0) oxidation [7,21,22]. The production of Cl_2 gas was also significantly inhibited by higher concentrations of SO_2 gas over metal oxides [14,23,24]. Recently, it was supposed that the Cl atom adsorbed onto coordinatively unsaturated ruthenium atoms might be enough and responsible

* Corresponding author. Tel.: +1 513 556 0018; fax: +1 413 556 0018.
E-mail address: joo.lee@uc.edu (J.-Y. Lee).

0926-3373/$ – see front matter © 2012 Elsevier B.V. All rights reserved.
http://dx.doi.org/10.1016/j.apcatb.2012.11.031

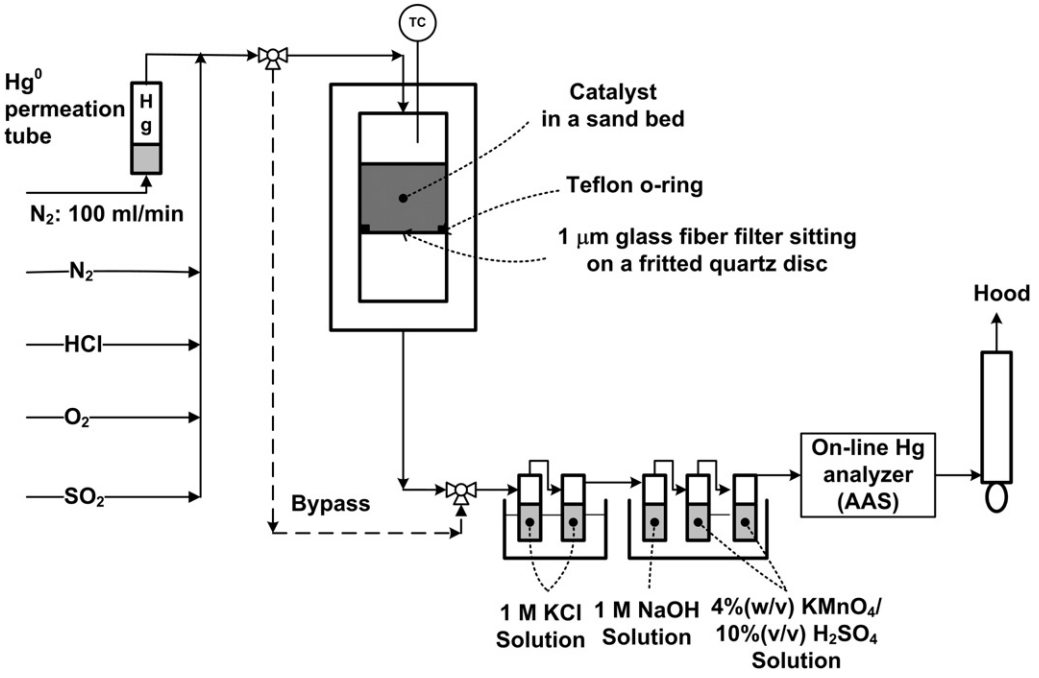

Fig. 1. A schematic of fixed-bed reactor.

for high Hg(0) conversion, suggesting a heterogeneous catalytic reaction [16]. The adsorption of HCl gas followed by the formation of Cl atoms onto metal oxide surfaces is thought to be the key to successful Hg(0) oxidation.

$$2HCl + \tfrac{1}{2}O_2 \leftrightarrow Cl_2 + H_2O \cdots \text{Deacon reaction},$$

$$\Delta H^0 = -28.4\,\text{kJ/mol} \quad (1)$$

It was reported that $CuCl_2/TiO_2$-based catalysts could simultaneously oxidize Hg(0) vapor and reduce NO gas but the NO reduction performance significantly decreased above 300–350 °C [25]. In our previous study, $CuCl_2$ was found to readily oxidize Hg(0) vapor but its resultant oxidized mercury is not easily adsorbed onto the non-carbonaceous substrate surface [26]. Carbon seems to be the only substrate that can effectively adsorb oxidized mercury. The resultant oxidized mercury species has recently been found to be primarily mercuric chloride ($HgCl_2$) using X-ray absorption fine structure (XAFS) spectroscopy [27]. Based on these findings, the primary objective of this study is to investigate the reaction mechanism of Hg(0) vapor oxidation over $CuCl_2$ under selected different gas conditions at 140 °C, targeting typical flue gas temperatures between the air preheater and electrostatic precipitator/fabric filter ranging between ~130 and ~180 °C [28].

2. Experimental

2.1. Catalyst preparation

There are many factors that can influence the performance of $CuCl_2$-based catalyst on Hg(0) oxidation such as $CuCl_2{\cdot}2H_2O$ loading, dispersion, copper speciation on different substrate, surface area, and pore volume. A $CuCl_2/\alpha$-Al_2O_3 catalyst was prepared by impregnating $CuCl_2{\cdot}2H_2O$ (Sigma, 97% purity) onto α-Al_2O_3 (Alfa Aesar aluminum oxide-43862, 1/8″ pellets, BET surface area = 0.25 m^2/g) in the aqueous phase following the incipient wetness method. In this study, non-porous α-Al_2O_3 was selected as a substrate, and 10% (wt) $CuCl_2$ (excluding the weight of $2H_2O$) was used throughout the study. α-Al_2O_3 is found to be inert toward copper speciation and not to react with $CuCl_2$ and form other copper compounds during $CuCl_2$ impregnation. In addition, while $CuCl_2/\gamma$-Al_2O_3 forms an amorphous form of $CuCl_2$, $CuCl_2$ formed onto α-Al_2O_3 was found to be in a crystalline form, allowing for the surface reactions between $CuCl_2$ and Hg(0) using X-ray diffraction (XRD). After impregnation, the samples were dried at 100 °C for 8 h. The synthesized catalyst was ground and sieved to ~40 μm particles for the characterization and performance evaluation of Hg(0) oxidation.

2.2. Performance evaluation of $CuCl_2/\alpha$-Al_2O_3 catalyst

A lab-scale fixed-bed system was used for the performance evaluation of Hg(0) oxidation and preparation of a spent catalyst for X-ray photoelectron spectroscopy (XPS) and X-ray diffraction (XRD) analysis. 25 mg of the catalyst was mixed with 4 g quartz sand and then was loaded into a fixed-bed reactor with an inner diameter of 12 mm. The length of reaction zone was ~20 mm. Before loading a catalyst, a blank test has been performed and showed negligible Hg(0) adsorption on the internal wall of either borosilicate reactor or Teflon tubing. The outlet mercury speciation was measured by the Ontario Hydro method. A 1 M KCl impinger solution was used to capture oxidized mercury. A 4% (w/v) $KMnO_4$/10% (v/v) H_2SO_4 impinger solution was used to capture Hg(0) vapor as shown in Fig. 1. Oxidized mercury and Hg(0) concentrations in the effluent gas stream were determined by analyzing those solutions using a cold vapor atomic absorption spectrophotometer (Model 400A, Buck Scientific Inc.). More detailed information on the system and experiments are described in our previous study [29]. The inlet Hg(0) concentration was 0.25 mg/N m^3 (=30 ppbv) in 1 L/min of a carrier gas flow, and the reactor was placed in an oven maintained at 140 °C. Four different gas conditions were used in this study: (1) N_2 (99.999% UHP, Wright Brothers, Inc.); (2) 6% O_2 (balanced with N_2); (3) 10 ppmv HCl and 6% O_2 (balanced with N_2); and (4) 2000 ppmv SO_2, 10 ppmv HCl, and 6% O_2 (balanced with N_2). When 2000 ppmv SO_2 was added, a 1 M NaOH solution was used to capture SO_2 gas, which was found to interfere with Hg(0) vapor captured in a 4% (w/v) $KMnO_4$/10% (v/v) H_2SO_4 impinger solution. When spent catalysts were prepared for characterization, the catalysts were not mixed with quartz sand and an inlet Hg(0) vapor

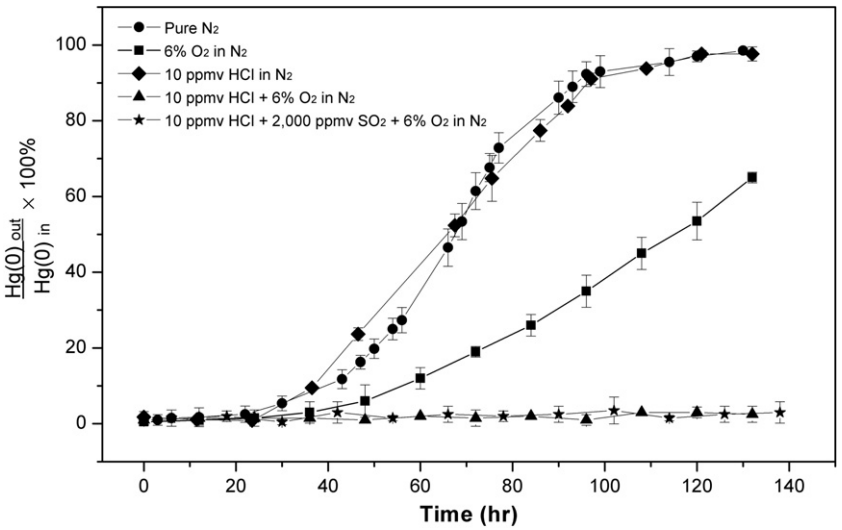

Fig. 2. Breakthrough curves of Hg(0) by 10% (wt) $CuCl_2/\alpha$-Al_2O_3 catalyst under different gas conditions at 140 °C.

concentration was raised to ~2 mg/N m^3 (=240 ppbv) in order to saturate the catalyst in a short period of time.

Another quartz reactor with a 6 mm inner diameter was used to examine Cl_2 gas generation over $CuCl_2/\alpha$-Al_2O_3 in a temperature-controlled tubular furnace (Model MTF 10/25/130, Carbolite Corp.). The fixed-bed system is very similar to the above fixed-bed reactor and the temperature of the reactor can be raised up to 1000 °C. 250 mL/min of a gas flow rate containing 10 ppmv HCl and 6% O_2 gases in N_2 gas was introduced to the reactor in order to keep the same velocity as that of the above fixed-bed reactor in a convection oven. The concentrations of HCl and Cl_2 gases were measured with specific gas detection tubes (Gastec).

2.3. Characterization

Thermal Gravimetric Analysis-Mass Spectrometry (TGA, TA Instruments TGA Q5000IR, and MS, Pfeiffer-Vacuum Thermostar) was used to evaluate the thermal stability of pure $CuCl_2$ and $CuCl_2/Al_2O_3$. Approximately 10 mg of a sample was used to ramp from room temperature to 800 °C with a heating rate of 5 °C/min under nitrogen flow (99.999% UHP) at a rate of 100 mL/min. The H_2-temperature programmed reduction (TPR) experiments were also performed using the Micromeritics Autochem 2910 automated catalyst characterization system with ~50 mg of samples. The samples were pretreated at 150 °C for 1 h in ultra-pure argon gas at a flow rate of 30 mL/min. After the furnace temperature decreased to ~50 °C, the feed gas (10%(v) H_2 balanced with Ar) was fed into the system at a flow rate of 30 mL/min. H_2-TPR runs were performed by heating the sample up to 600 °C at a linear heating rate of 6.5 °C/min. The amount of hydrogen gas consumed during the TPR experiment was measured by a built-in thermal conductive detector (TCD). XPS (Kratos Axis Ultra, with a monochromated Al Kα source (1486.6 eV)) measurements were used to examine copper speciation with a concentric hemispherical analyzer. The power applied to the X-ray gun was 130 W (I = 10 mA, V = 13 kV), and the base vacuum pressure was 1×10^{-7} Torr, and the pass energy of the analyzer was set to 20 eV. The resolution of the spectra was ~0.2 eV with the step size of 0.1 eV. The carbon 1s peak at 284.5 eV was used to charge reference all binding energies. XRD data were obtained using Cu Kα radiation with a wavelength of 1.5406 Å (X'Pert Pro MPD X-ray diffractometer). An aluminum holder was used to support the catalyst samples. The scanning range was from 10° to 60° (2θ) with a step size of 0.02° and a step time of 0.5 s.

3. Results and discussion

3.1. Hg(0) oxidation over $CuCl_2/\alpha$-Al_2O_3 catalyst

The Hg(0) oxidation over the 10% (wt) $CuCl_2/\alpha$-Al_2O_3 catalyst evaluated under different gas conditions are shown in Fig. 2, and their mercury mass balances are summarized in Table 1. Before the performance evaluation, it was confirmed that unsupported α-Al_2O_3 did not adsorb Hg(0) vapor at 140 °C. The mercury mass balance closures obtained from the impinger analysis are found to be within ~±3.1% of the inlet Hg(0) concentration. A spent catalyst obtained under pure N_2 flow was analyzed for the amount of mercury adsorption to ensure the above gas-phase mercury mass balance by following the digestion procedures described in the Ontario Hydro method. The amount of mercury determined from the digestion of the spent catalyst was found to be less than 0.2% of the total amount of inlet Hg(0) added over the evaluation period, all of which indicate that the adsorption of both Hg(0) and oxidized mercury (hereafter Hg(2+)) onto the internal surfaces of the reactor system is negligible and almost all mercury left the reactor system. The results clearly show that the catalyst can oxidize almost all Hg(0) vapor during the first 24 h under any carrier gas conditions. The 10% (wt) $CuCl_2/\alpha$-Al_2O_3 catalyst lost its oxidation capability after ~120 h under a nitrogen carrier gas. Based on the molecular weight of $CuCl_2$ (MW = 134.5) and 30 ppbv Hg(0) vapor in 1 L/min of a total flow rate, the Hg(0) oxidation reaction is estimated to be complete with $CuCl_2$ in ~120 h when the reaction takes place at a stoichiometric ratio of 2 between $CuCl_2$ and Hg(0) (i.e. $2CuCl_2$:Hg(0)). This mercury speciation result also corresponds to our previous result obtained from $CuCl_2$ doped onto activated carbon [30].

When Hg(0) vapor was introduced in N_2 and O_2 gases, O_2 gas was found to have a capability to promote Hg(0) oxidation compared to N_2 gas. However, the Hg(0) oxidation started to decrease and eventually stopped under both carrier gases. When 10 ppmv HCl gas was added to N_2 gas, Hg(0) oxidation was gradually attenuated, similar to the performance shown in N_2 gas. However, an interesting result was obtained when O_2 gas was added to the HCl gas. Hg(0) vapor continued to almost completely be oxidized in 10 ppmv HCl and 6% (v) O_2 gases balanced with N_2 gas, even in the presence of 2000 ppmv SO_2 gas over 140 h of the performance evaluations. These results indicate that $CuCl_2/\alpha$-Al_2O_3 catalyst requires both HCl and O_2 gases for Hg(0) oxidation and also has excellent resistance to SO_2. SO_2 gas has been reported to adversely affect Hg(0) oxidation over many metal oxide-based catalysts

Table 1
Mercury speciation results from 10% (wt) $CuCl_2/\alpha$-Al_2O_3 fixed-bed tests. Inlet Hg^0 concentration = 30 ± 2 ppbv.

Under N_2	Time (h)	0	3	22	47	72	96	120
	Hg species (%)							
	Inlet Hg^0	100	100	100	100	100	100	100
	Outlet Hg^0	0	0	3 ± 1	16 ± 2	62 ± 3	93 ± 3	97 ± 2
	Outlet Hg^{2+}	92 ± 2	96 ± 2	93 ± 2	79 ± 2	36 ± 2	8 ± 2	2 ± 2
	Total outlet Hg	92 ± 2	96 ± 2	96 ± 3	95 ± 3	98 ± 4	101 ± 4	99 ± 3
Under 6%(v) O_2	Time (h)	0	12	24	48	72	96	120
	Hg species (%)							
	Inlet Hg^0	100	100	100	100	100	100	100
	Outlet Hg^0	0	1 ± 1	2 ± 1	6 ± 3	19 ± 2	35 ± 4	54 ± 4
	Outlet Hg^{2+}	94 ± 2	97 ± 3	94 ± 3	91 ± 2	79 ± 3	67 ± 2	45 ± 2
	Total outlet Hg	94 ± 2	98 ± 4	96 ± 4	97 ± 4	98 ± 4	102 ± 5	99 ± 5
Under 10 ppmv HCl in N_2	Time (h)	0	12	36	68	86	109	132
	Hg species (%)							
	Inlet Hg^0	100	100	100	100	100	100	100
	Outlet Hg^0	2 ± 2	1 ± 1	9 ± 2	52 ± 3	77 ± 3	94 ± 1	98 ± 2
	Outlet Hg^{2+}	99 ± 3	99 ± 4	95 ± 3	50 ± 2	24 ± 2	8 ± 1	1 ± 1
	Total outlet Hg	101 ± 4	100 ± 5	104 ± 4	102 ± 4	101 ± 4	102 ± 2	99 ± 3
Under 6%(v) O_2 + 10 ppmv HCl in N_2	Time (h)	0	12	24	48	72	96	120
	Hg species (%)							
	Inlet Hg^0	100	100	100	100	100	100	100
	Outlet Hg^0	0	1 ± 1	2 ± 1	1 ± 1	2 ± 1	1 ± 1	3 ± 1
	Outlet Hg^{2+}	94 ± 3	97 ± 2	94 ± 1	96 ± 2	96 ± 3	100 ± 2	96 ± 3
	Total outlet Hg	94 ± 3	98 ± 3	96 ± 2	97 ± 3	98 ± 4	101 ± 3	99 ± 4
Under O_2, 10 ppmv HCl + 2000 ppmv SO_2 in N_2	Time (h)	6	18	36	54	78	102	126
	Hg species (%)							
	Inlet Hg^0	100	100	100	100	100	100	100
	Outlet Hg^0	1 ± 1	2 ± 1	0	2 ± 1	2 ± 1	3 ± 2	2 ± 1
	Outlet Hg^{2+}	95 ± 4	95 ± 2	96 ± 1	95 ± 2	99 ± 2	97 ± 2	97 ± 3
	Total outlet Hg	96 ± 5	97 ± 3	96 ± 1	97 ± 3	101 ± 3	100 ± 3	99 ± 4

[14,23,24]. These notable performance differences in Hg(0) oxidation over the $CuCl_2/\alpha$-Al_2O_3 catalyst under different gas conditions prompted us to study the following Hg(0) oxidation mechanisms.

3.2. Characterization results of $CuCl_2/\alpha$-Al_2O_3 catalyst

3.2.1. BET surface area and pore volume analysis

The original α-Al_2O_3 pellet comprising powders has a macropore structure with very small surface area (0.25 m^2/g) and pore volume (0.26 mL/g). The α-alumina powder is primarily a nonporous material with external surface areas, and makes it easy to study the oxidation state of copper by XPS that can probe a few nanometers below the surface.

3.2.2. TGA-MS analysis

The thermal stability of unsupported CuCl, $CuCl_2{\cdot}2H_2O$ and $CuCl_2/\alpha$-Al_2O_3 catalyst was examined by TGA-MS, and the results are shown in Fig. 3. The early weight loss of 21% before 100 °C from both pure $CuCl_2{\cdot}2H_2O$ and $CuCl_2/\alpha$-Al_2O_3 is derived from the evaporation of dihydrate. Then both samples lost all weight between ~350 and 550 °C where chlorine evolution was detected by MS. Unsupported CuCl lost most of the weight between ~410 and 560 °C, but chlorine release was not detected by MS. Pure CuCl is known to melt and vaporize at ~420 °C, and the CuCl vapor is too heavy to reach the MS capillary tube inlet. These results indicate that dehydrated $CuCl_2$ loses additional 21% by releasing chlorine and turns into CuCl at 438 °C and then the remaining CuCl starts to evaporate without any chlorine release. Since alumina is thermally very stable up to 800 °C, the 10% (wt) $CuCl_2/\alpha$-Al_2O_3 sample lost all $CuCl_2$ (i.e. 10% weight) during the ramping process.

3.2.3. TPR analysis

The H_2-TPR profiles for $CuCl_2/\alpha$-Al_2O_3, $CuCl_2{\cdot}2H_2O$, and CuCl shown in Fig. 4 were obtained in order to evaluate the redox performance of the $CuCl_2/\alpha$-Al_2O_3 catalyst in terms of temperature. The TPR profiles for unsupported $CuCl_2{\cdot}2H_2O$ and CuCl (Sigma, 97% purity) show two peaks: one major peak at ~430 °C and one minor peak at ~550 °C for $CuCl_2{\cdot}2H_2O$; and one minor peak at ~380 °C and one major peak at ~550 °C for CuCl. The first low-temperature major peak for $CuCl_2{\cdot}2H_2O$ results from the reduction of Cu(II) to Cu(I), and the second minor peak is derived from the reduction of Cu(I) to Cu(0). The CuCl TPR profile shows a low-temperature minor peak and a high-temperature major peak. The low-temperature minor peak indicates the reduction of Cu(II) to Cu(I), and seems to come from a Cu(II) species included in the unsupported CuCl sample with 97% purity. On the other hand, the 10% (wt)

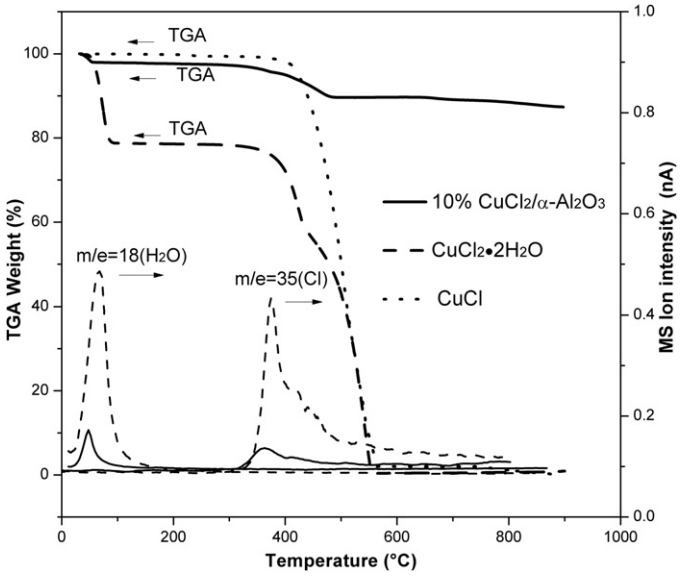

Fig. 3. TGA-MS results for $CuCl_2{\cdot}2H_2O$, CuCl and 10% (wt) $CuCl_2/\alpha$-Al_2O_3 catalyst.

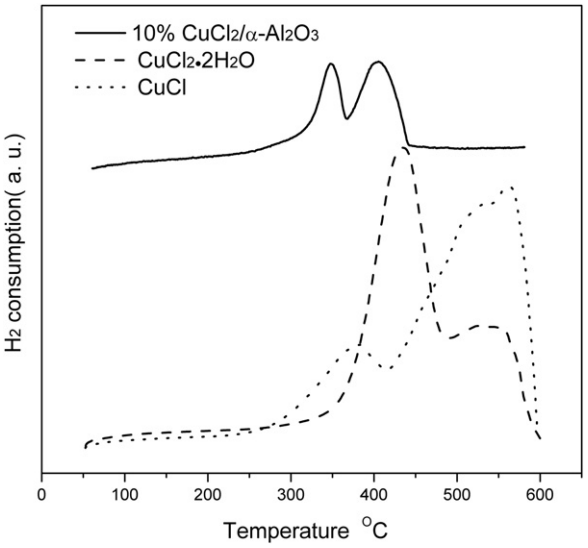

Fig. 4. H_2-TPR profiles for 10% (wt) $CuCl_2/\alpha$-Al_2O_3, $CuCl_2$, and CuCl.

$CuCl_2/\alpha$-Al_2O_3 catalyst showed two distinct peaks at the temperatures lower than unsupported $CuCl_2{\cdot}2H_2O$ and CuCl, which is in agreement with the results reported in a previous study [31]. The lower copper reduction temperature for the supported catalyst may be derived from the increased surface/volume ratio compared to unsupported $CuCl_2{\cdot}2H_2O$. The low- and high-temperature peaks indicate the two-step reduction of Cu(II) to Cu(I) and Cu(I) to Cu(0), respectively.

3.2.4. XRD analysis

As presented in the performance evaluation section, the $CuCl_2/\alpha$-Al_2O_3 sample can oxidize Hg(0) vapor regardless of the presence of O_2 and HCl gases. In order to investigate the Hg(0) oxidation mechanism, XRD and XPS techniques were employed to identify the copper compounds in the crystalline phase and to examine the oxidation state of copper during the Hg(0) oxidation process. First, the XRD patterns of several samples including unsupported $CuCl_2{\cdot}2H_2O$, CuCl, Al_2O_3 substrate, fresh $CuCl_2/\alpha$-Al_2O_3, and spent $CuCl_2/\alpha$-Al_2O_3 prepared in different Hg(0)-laden gases were examined as shown in Fig. 5. The XRD pattern of the fresh 10% (wt) $CuCl_2/\alpha$-Al_2O_3 sample was superimposed on those of $CuCl_2{\cdot}2H_2O$ and α-Al_2O_3, indicating that the impregnated $CuCl_2{\cdot}2H_2O$ predominantly has its original crystalline $CuCl_2{\cdot}2H_2O$ structure (Fig. 5a). On the other hand, the spent $CuCl_2/\alpha$-Al_2O_3 showed a distinguishable difference in the XRD pattern. In N_2 flow (Fig. 5b), the peaks derived from $CuCl_2{\cdot}2H_2O$ became attenuated, and the CuCl peaks started to appear, indicating that the $CuCl_2{\cdot}2H_2O$ on alumina was converted into CuCl as Hg(0) vapor reacted with $CuCl_2$. On the other hand, when 10 ppmv HCl and 6% (v) O_2 were used in N_2 flow (Fig. 5c and d), CuCl peaks became weak at $2\theta = 28.9^\circ$ and disappeared at 47.2° and 56.1° while $CuCl_2{\cdot}2H_2O$ peaks were as noticeable as the fresh catalyst shown in Fig. 5a. The presence of 2000 ppmv SO_2 did not give any noticeable difference in XRD patterns, substantiating that SO_2 does not give an impact on Hg(0) oxidation over $CuCl_2/\alpha$-Al_2O_3.

$CuCl_2$ has been studied as a catalyst for Cl_2 production via HCl oxidation in the presence of O_2 and HCl called the Deacon or Deacon-like reaction [32]. In order to further investigate a regeneration possibility of CuCl, fresh CuCl exposed to only O_2 and both HCl and O_2 gases was also examined with XRD. Upon the exposure of fresh CuCl to only O_2 gas (Fig. 5e), two new peaks appeared at $2\theta = 17.6^\circ$ and 35.6°, and were identified to belong to a copper oxychloride species, Cu_2OCl_2 (PDF-ICDD 01-072-6749). When

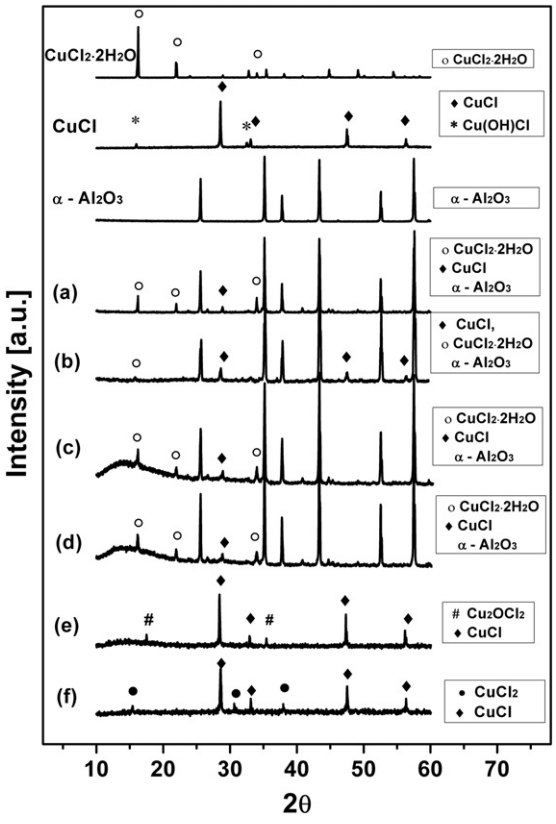

Fig. 5. X-ray diffraction patterns of $CuCl_2/\alpha$-Al_2O_3 obtained under different gases, (a) fresh 10% $CuCl_2/\alpha$-Al_2O_3; (b) spent 10% $CuCl_2/\alpha$-Al_2O_3 (carrier gas: N_2); (c) spent 10% $CuCl_2/\alpha$-Al_2O_3 (carrier gas: 6% O_2 + 10 ppmv HCl in N_2); (d) spent 10% $CuCl_2/\alpha$-Al_2O_3 (carrier gas: 6% (v) O_2 + 10 ppmv HCl + 2000 ppmv SO_2 in N_2); (e) spent CuCl (treated in O_2); (f) spent CuCl (treated in 10 ppmv HCl + O_2).

fresh CuCl was treated under 10 ppmv HCl in O_2 gas (Fig. 5f), an anhydrated $CuCl_2$ phase (PDF-ICDD 01-074-0974) was identified from the spent CuCl sample, suggesting a re-chlorination possibility.

3.2.5. XPS analysis

XPS characterization was also used to examine the copper speciation over the $CuCl_2/\alpha$-Al_2O_3 catalyst. Fig. 6 shows the high resolution Cu $2p_{3/2}$ XPS characterization result for unsupported $CuCl_2$, CuCl, and 10% $CuCl_2/\alpha$-Al_2O_3 catalyst before and after Hg(0) oxidation. The standard fresh $CuCl_2$ and CuCl XPS profiles show that the Cu $2p_{3/2}$ characteristic binding energy is 934.5 eV for Cu(II) in $CuCl_2$, and 931.5 eV for Cu(I) in CuCl, respectively. When the XPS result for a fresh $CuCl_2/\alpha$-Al_2O_3 sample is compared with that for fresh $CuCl_2$ and CuCl samples, the oxidation state of copper in the fresh $CuCl_2/\alpha$-Al_2O_3 sample is found to be predominantly Cu(II) with little Cu(I) (Fig. 6a). However, after Hg(0) oxidation in N_2 gas (Fig. 6(b_1) & (b_2)), the major copper oxidation state of the spent $CuCl_2/\alpha$-Al_2O_3 sample turned out to be Cu(I), and the Cu(II) oxidation peak intensity started to be attenuated as the Hg(0) reaction time increased. It is interesting to note that an XPS result obtained from a spent $CuCl_2/\alpha$-Al_2O_3 sample under 10 ppmv HCl in O_2 gas (Fig. 6c) showed primarily the Cu(II) oxidation state of $CuCl_2$. These XPS results also suggest that $CuCl_2$ is converted into CuCl during Hg(0) oxidation in N_2 flow, but $CuCl_2$ can continue to be regenerated for Hg(0) oxidation in 10 ppmv HCl in O_2 gas. In addition, the presence of 2000 ppmv SO_2 did not make any significant difference (Fig. 6d).

A spent CuCl sample was also examined for XPS after being treated with O_2 (Fig. 6e) and 10 ppmv HCl in O_2 flow (Fig. 6f). Upon

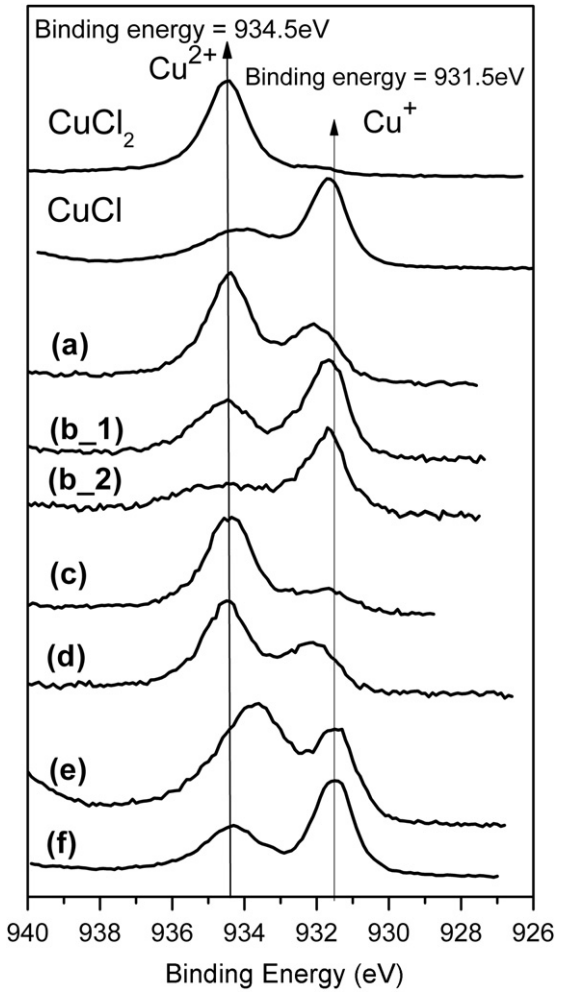

Fig. 6. Cu $2p_{3/2}$ high resolution XPS results for 10% $CuCl_2/\alpha$-Al_2O_3 obtained before and after Hg(0) oxidation under different gases. (a) Fresh 10% $CuCl_2/\alpha$-Al_2O_3; (b_1) spent 10% $CuCl_2/\alpha$-Al_2O_3 (carrier gas: N_2, after 30 h); (b_2) spent 10% $CuCl_2/\alpha$-Al_2O_3 (carrier gas: N_2, after 60 h); (c) spent 10% $CuCl_2/\alpha$-Al_2O_3 (carrier gas: 6% (v) O_2 + 10 ppmv HCl, after 30 h); (d) spent 10% $CuCl_2/\alpha$-Al_2O_3 (carrier gas: 6% (v) O_2 + 10 ppmv HCl + 2000 ppmv SO_2, after 30 h); (e) spent CuCl (treated in 6% (v) O_2, after 30 h); (f) spent CuCl (treated in 10 ppmv HCl in 6% (v) O_2, after 30 h).

the exposure of CuCl to O_2 gas, most Cu(I) was turned into Cu(II). However, the binding energy peak for Cu(II) appears at 933.5 eV, and is slightly different from the binding energy peak of 934.5 eV for $CuCl_2$. The Cu(II) peak may be derived from a copper species associated with an oxygen atom, such as Cu_2OCl_2 found from the above XRD examination. However, the XPS peak position could not be used to identify the copper species since many copper compounds with the Cu(II) oxidation state appear at a nearby binding energy. There is a general agreement on a hypothesis that CuCl forms Cu_2OCl_2 by oxidation with O_2 gas and is subsequently converted into $CuCl_2$ with HCl gas [32,33]. However, it is not completely clear at this moment how Hg(0) oxidation is promoted over $CuCl_2$ by O_2 gas as shown in Fig. 2. On the other hand, a CuCl sample exposed to 10 ppmv HCl in O_2 gas for 30 h shows the Cu(II) peak matching with that of $CuCl_2$.

Table 2 shows a change in atomic ratios during the Hg(0) reaction over $CuCl_2/\alpha$-Al_2O_3 determined from an XPS curve fitting method based on all Cu 2p peaks. After 60 h of the Hg(0) reaction, an atomic ratio of Cu to Cl decreased from 1:2 to 1:1.1 while almost all Cu(II) was converted into Cu(I). The Cl content on the spent sample decreased because Cl was consumed to oxidize Hg(0) vapor and the resultant $HgCl_2$ did not adsorb and sublimed the sample. This result also supports the conversion of $CuCl_2$ into CuCl during the reaction. All of these XPS results are in a good agreement with the above XRD results.

3.3. Heterogeneous catalytic oxidation of Hg(0) vapor over $CuCl_2$

As shown in reaction (1), the overall Deacon reaction is an exothermic reaction. The HCl uptake reaction is exothermic and thermodynamically favorable at low temperatures between 100 and 250 °C [33]. However, the Cl_2 release step is endothermic and favors a high-temperature window between 300 and 360 °C. Thus in an efficient two-stage HCl oxidation process, a $CuCl_2$-based catalyst is typically operated in the elevated temperature range for Cl_2 production. In order to examine a possibility of homogeneous Hg(0) oxidation, Cl_2 gas concentrations were measured at the outlet of the quartz reactor in the tubular furnace by introducing 10 ppmv HCl and 6% O_2 gases in N_2 gas to the reactor containing $CuCl_2/\alpha$-Al_2O_3. The same 10 ppmv HCl concentration was detected at the inlet and outlet of the reactor, and no Cl_2 gas was detected using a Cl_2 gas detection tube with a 0.1 ppm detection limit at 140 and 200 °C. However, when 10 ppmv HCl and 6% O_2 gases in N_2 gas were introduced to the reactor at 300 °C, 18 ppmv Cl_2 gas was detected 10 min after the gases were introduced. Considering a 2:1 stoichiometric ratio of HCl:Cl_2 gases, 5 ppmv Cl_2 gas should be generated if all Cl_2 gas is derived from the HCl conversion. This indicates that the evolution of Cl_2 gas at 300 °C results from both of $CuCl_2$ decomposition and HCl conversion. However, the result clearly demonstrates that Hg(0) vapor reacts with Cl atoms in $CuCl_2$ at 140 °C via heterogeneous reaction.

The XRD and XPS results for $CuCl_2/\alpha$-Al_2O_3 samples presented above clearly show that the $CuCl_2$ impregnated onto α-Al_2O_3 exists in the same crystalline structure as unsupported $CuCl_2$, and has a capability to oxidize Hg(0) vapor. It was found that Hg(0) vapor reacts with atomic chlorine of $CuCl_2$ for Hg(0) oxidation, and $CuCl_2$ is reduced to CuCl via reaction (2). This suggests that Hg(0) oxidation over $CuCl_2$ should take place via a Mars–Maessen mechanism by which Hg(0) vapor adsorbed onto the $CuCl_2$ surface would react with atomic Cl on $CuCl_2$ [7]. The oxidized mercury species formed as a result of the reaction of Hg(0) vapor with $CuCl_2$ was primarily mercuric chloride ($HgCl_2$) regardless of the presence of HCl and O_2 gases [27]. However, both HCl and O_2 gases were found to be required for the reduced CuCl to be re-chlorinated back to $CuCl_2$ via intermediate copper oxychloride (Cu_2OCl_2) formation as shown in reactions (3) and (4). Based on these results, $CuCl_2$ was found to work as a redox catalyst that oxidizes Hg(0) vapor and reduces itself to CuCl while the reduced CuCl is re-oxidized to $CuCl_2$ via the overall reaction (5).

$$Hg(0) + 2CuCl_2 \rightarrow HgCl_2 + 2CuCl \quad (2)$$

$$2CuCl + \tfrac{1}{2}O_2 \rightarrow Cu_2OCl_2 \quad (3)$$

$$Cu_2OCl_2 + 2HCl \rightarrow 2CuCl_2 + H_2O \quad (4)$$

$$\text{Overall}: Hg(0) + 2HCl + \tfrac{1}{2}O_2 \xrightarrow{CuCl_2} HgCl_2 + H_2O \quad (5)$$

It is interesting to note that both HCl and O_2 gases were found to be required to replenish the empty Cl lattices in $CuCl_2$ while Cl atoms in occupied lattices are consumed for the oxidation of Hg(0) vapor to $HgCl_2$ and Cl_2 gas liberation is suppressed in low temperatures such as 140 and 200 °C. This is similar to the first step of HCl oxidation to Cl of the Deacon reaction used for oxychlorination, but is different from the reaction in that Cl_2 gas is not liberated at these low temperatures. The performance evaluation results clearly show that atomic Cl formed on the surface as a result of the HCl oxidation is sufficient for the replenishment of empty Cl lattices due to a large (i.e. three orders of magnitude)

Table 2
Results of quantitative XPS analysis for 10%(wt) $CuCl_2/\alpha$-Al_2O_3.

Samples	Atomic ratio of Cu^{2+} to Cu^{1+}	Atomic ratio of Cu to Cl	Atomic ratio of O to Al
Unsupported CuCl		1:1	Not applicable
Unsupported $CuCl_2$		1:2	Not applicable
(a) Fresh 10% $CuCl_2/\alpha$-Al_2O_3	4:1	1:2	3:2
(b_1) Spent 10% $CuCl_2/\alpha$-Al_2O_3 (carrier gas: N_2, after 30 h)	0.5:1	1:1.5	3:2
(b_2) Spent 10% $CuCl_2/\alpha$-Al_2O_3 (carrier gas: N_2, after 60 h)	0.2:1	1:1.1	3:2
(c) Spent 10% $CuCl_2/\alpha$-Al_2O_3 (carrier gas: 6%(v) O_2 + 10 ppmv HCl, after 30 h)	8:1	1:2	3:2
(d) Spent 10% $CuCl_2/\alpha$-Al_2O_3 (carrier gas: 6%(v) O_2 + 10 ppmv HCl + 2000 ppmv SO_2, after 30 h)	4:1	1:2	3:2
(e) Spent CuCl (treated in 6%(v) O_2, after 30 h)	3:1	1:1	Not applicable
(f) Spent CuCl (treated in 10 ppmv HCl in 6%(v) O_2, after 30 h)	0.4:1	1:1.2	Not applicable

concentration difference between HCl gas and Hg(0) vapor, which allows for continuous Hg(0) vapor oxidation over $CuCl_2$. These findings suggest that a primary Hg(0) oxidation mechanism over $CuCl_2$ surfaces is a heterogeneous reaction and surface Cl is responsible for the Hg(0) oxidation. The prechlorinated sites of $CuCl_2$ were reported to have a propensity for surface chlorination derived from HCl oxidation for the Deacon reaction [32,34]. However, the rechlorination step under various flue gas components seems to be the key to the success of the $CuCl_2$-based catalyst for Hg(0) oxidation.

4. Conclusions

$CuCl_2$ was found to work as an excellent redox catalyst for heterogeneous Hg(0) oxidation at 140 °C by reducing itself to CuCl, and to be reoxidized back to $CuCl_2$ with HCl and O_2 gases typically present in coal combustion flue gases. Unlike many metal oxide-based catalysts, $CuCl_2$ also showed excellent resistance to SO_2 for Hg(0) vapor oxidation. However, the thermal decomposition of $CuCl_2$ is likely to limit the application at high temperatures above ~300 °C. The actual gas hourly space velocity inside the fixed-bed reactor used in this study was ~40,000 h^{-1} at 140 °C and was high enough to be realized in a honeycomb or plate catalyst bed. The effects of temperatures and various flue gas constituents on Hg(0) vapor oxidation over $CuCl_2$ are planning to be investigated.

Acknowledgements

This study was primarily funded by the University of Cincinnati through faculty start-up funds and partly funded by the National Science Foundation, NSF CAREER Grant # 1151017. The authors greatly appreciate their financial support.

Appendix A. Supplementary data

Supplementary data associated with this article can be found, in the online version, at http://dx.doi.org/10.1016/j.apcatb.2012.11.031.

References

[1] National Emission Standards for Hazardous Air Pollutants From Coal- and Oil-Fired Electric Utility Steam Generating Units and Standards of Performance for Fossil-Fuel-Fired Electric Utility, Industrial-Commercial-Institutional, and Small Industrial-Commercial-Institutional Steam Generating Units; Proposed Rule. 40 CFR Parts 60 and 63. Federal Register 77:32 (16.2.12), p. 24976.
[2] Federal Implementation Plans To Reduce Interstate Transport of Fine Particulate Matter and Ozone. 40 CFR Parts 51, 52, 72, 78, and 97. Federal Register 75:147 (2.8.10), p. 45210.
[3] Federal Implementation Plans To Reduce Interstate Transport of Fine Particulate Matter and Ozone; Correction. 40 CFR Parts 51, 52, 72, 78, and 97. Federal Register 75:177 (14.9.10), p. 45210.
[4] U.S. Environmental Protection Agency, Integrated Planning Model (IPM) v.4.10 Model Runs, U.S. Environmental Protection Agency, 2010.
[5] U.S. Department of Energy, Annual Energy Outlook 2007 with Projections to 2030, Energy Information Administration, 2007.
[6] A.P. Jones, J.W. Hoffmann, D.N. Smith, T.J. Feeley, J.T. Murphy, Environmental Science & Technology 41 (2007) 1365–1371.
[7] A.A. Presto, E.J. Granite, Environmental Science & Technology 40 (2006) 5601–5609.
[8] R.K. Srivastava, N. Hutson, B. Martin, F. Princiotta, J. Staudt, Environmental Science & Technology 40 (2006) 1385–1393.
[9] D.R. Lide, CRC Handbook Chemistry and Physics, 85th ed., CRC Press, Boca Raton, FL, 2004.
[10] Y. Zhao, M.D. Mann, J.H. Pavlish, B.A.F. Mibeck, G.E. Dunham, E.S. Olson, Environmental Science & Technology 40 (2006) 1603–1608.
[11] J.A. Hrdlicka, W.S. Seames, M.D. Mann, D.S. Muggli, C.A. Horabik, Environmental Science & Technology 42 (2008) 6677–6682.
[12] A.A. Presto, E.J. Granite, Platinum Metals Review 52 (2008) 144–154.
[13] H. Kamata, S.-i. Ueno, N. Sato, T. Naito, Fuel Processing Technology 90 (2009) 947–951.
[14] J. Li, N. Yan, Z. Qu, S. Qiao, S. Yang, Y. Guo, P. Liu, J. Jia, Environmental Science & Technology 44 (2010) 426–431.
[15] Y. Liu, Y. Wang, H. Wang, Z. Wu, Catalysis Communications 12 (2011) 1291–1294.
[16] N. Yan, W. Chen, J. Chen, Z. Qu, Y. Guo, S. Yang, J. Jia, Environmental Science & Technology 45 (2011) 5725–5730.
[17] S. Straube, T. Hahn, H. Koeser, Applied Catalysis B: Environmental 79 (2008) 286–295.
[18] H. Li, C.-Y. Wu, Y. Li, J. Zhang, Applied Catalysis B: Environmental 111/112 (2012) 381–388.
[19] S. Yang, Y. Guo, N. Yan, D. Wu, H. He, J. Xie, Z. Qu, J. Jia, Applied Catalysis B: Environmental 101 (2011) 698–708.
[20] Y. Cao, Z. Gao, J. Zhu, Q. Wang, Y. Huang, C. Chiu, B. Parker, P. Chu, W.-P. Pan, Environmental Science & Technology 42 (2008) 256–261.
[21] S. Niksa, N. Fujiwara, Journal of the Air & Waste Management Association 55 (2005) 930–939.
[22] J. Wang, E.J. Anthony, Chemical Engineering & Technology 28 (2005) 569–573.
[23] S. Qiao, J. Chen, J. Li, Z. Qu, P. Liu, N. Yan, J. Jia, Industrial & Engineering Chemistry Research 48 (2009) 3317–3322.
[24] Y. Cao, B. Chen, J. Wu, H. Cui, J. Smith, C.-K. Chen, P. Chu, W.-P. Pan, Energy & Fuels 21 (2007) 145–156.
[25] M.H. Kim, S.-W. Ham, J.-B. Lee, Applied Catalysis B: Environmental 99 (2010) 272–278.
[26] S.-S. Lee, J.-Y. Lee, T.C. Keener, Journal of the Chinese Institute of Chemical Engineers 39 (2008) 137–142.
[27] X. Li, J.-Y. Lee, S. Heald, Fuel 93 (2012) 618–624.
[28] A. Pakrasi, W.T. Davis, in: W.T. Davis (Ed.), Air & Waste Management Association (2000) 191–221.
[29] J.-Y. Lee, Y.H. Ju, T.C. Keener, R.S. Varma, Environmental Science & Technology 40 (2006) 2714–2720.
[30] S.-S. Lee, J.-Y. Lee, T.C. Keener, Fuel Processing Technology 90 (2009) 1314–1318.
[31] A.J. Rouco, Applied Catalysis A: General 117 (1994) 139–149.
[32] A.P. Amrute, C. Mondelli, M.A.G. Hevia, J. Perez-Ramirez, The Journal of Physical Chemistry C 115 (2011) 1056–1063.
[33] H.Y. Pan, R.G. Minet, S.W. Benson, T.T. Tsotsis, Industrial & Engineering Chemistry Research 33 (1994) 2996–3003.
[34] A.P. Amrute, C. Mondelli, M.A.G. Hevia, J. Perez-Ramirez, ACS Catalysis 1 (2011) 583–590.